



EARTHQUAKE ENGINEERING INTENSITY SCALE: A TEMPLATE WITH MANY USES

Sigmund A. FREEMAN¹, Ayhan IRFANOGLU², and Terrence F. PARET³

SUMMARY

The Earthquake Engineering Intensity Scale (EEIS) is a building shaking intensity measure that has been developed along the lines of the Engineering Intensity Scale of the late John A. Blume. This measure, which is in fact a graphical template, allows translation of ground shaking information in the form of response spectra at a site into response/shaking intensity for different kinds of buildings. EEIS can be used as a tool for several purposes, such as: 1) to graphically illustrate damage potential of ground motions; 2) to rapidly identify vulnerable building types after an earthquake; 3) to assess capacity of buildings; 4) to facilitate incorporation of earthquake ground motion and building response data. The EEIS concept also allows tracking the evolution of building code strength requirements. This paper describes the concept of the EEIS and uses a sampling of strong earthquake ground motions with varying characteristics to illustrate some of its uses. The template is also used to provide a chronology of U.S. building code development from its design spectra perspective.

INTRODUCTION

In the 1970s, in anticipation of possible peaceful use of nuclear arms, John A. Blume developed the Engineering Intensity Scale to monitor building damage potential of nuclear and chemical explosions [1]. Naturally, he suggested that the scale was applicable to earthquake motions as well. His scale utilized response spectra presented in the form of pseudo relative response velocity versus period. Traditionally, though, earthquake intensity measures depend on post-event observations of damage and the absence of damage, and not on any particular ground motion parameter. With the advent of and recordings by dense strong ground motion arrays, large-scale regression studies have been made to develop analytical correlation formulations between traditional earthquake intensity measures, such as Modified Mercalli Intensity (MMI) scale [2], and peak ground motion parameters, such as peak ground acceleration (PGA) and peak ground velocity (PGV). In particular, in the United States, the development of TriNet ShakeMaps brought the automated and rapid ground shaking intensity estimation into wide application [3]. Identifying the damage potential of different parameters obtained from ground motions [4], regression relationships between Instrumental Intensity, I_{mm} , (which is proxy for MMI obtained from data recorded

¹ Principal, Wiss, Janney, Elstner Assoc., Inc., Emeryville, CA, USA. Email: SFreeman@wje.com

² Associate III, Wiss, Janney, Elstner Assoc., Inc., Emeryville, CA, USA. Email: AIrfanoglu@wje.com

³ Senior Consultant, Wiss, Janney, Elstner Assoc., Inc., Emeryville, CA, USA. Email: TParet@wje.com

by stations), and the PGA and PGV were developed. These analytical expressions, which were based on data from eight southern California earthquakes, resulted in the PGA-PGV range-pairs and I_{mm} values as shown in the table in Figure 1. The relationship and a color-coded I_{mm} map for the 1994 Northridge earthquake in the Los Angeles area is shown in Figure 1.

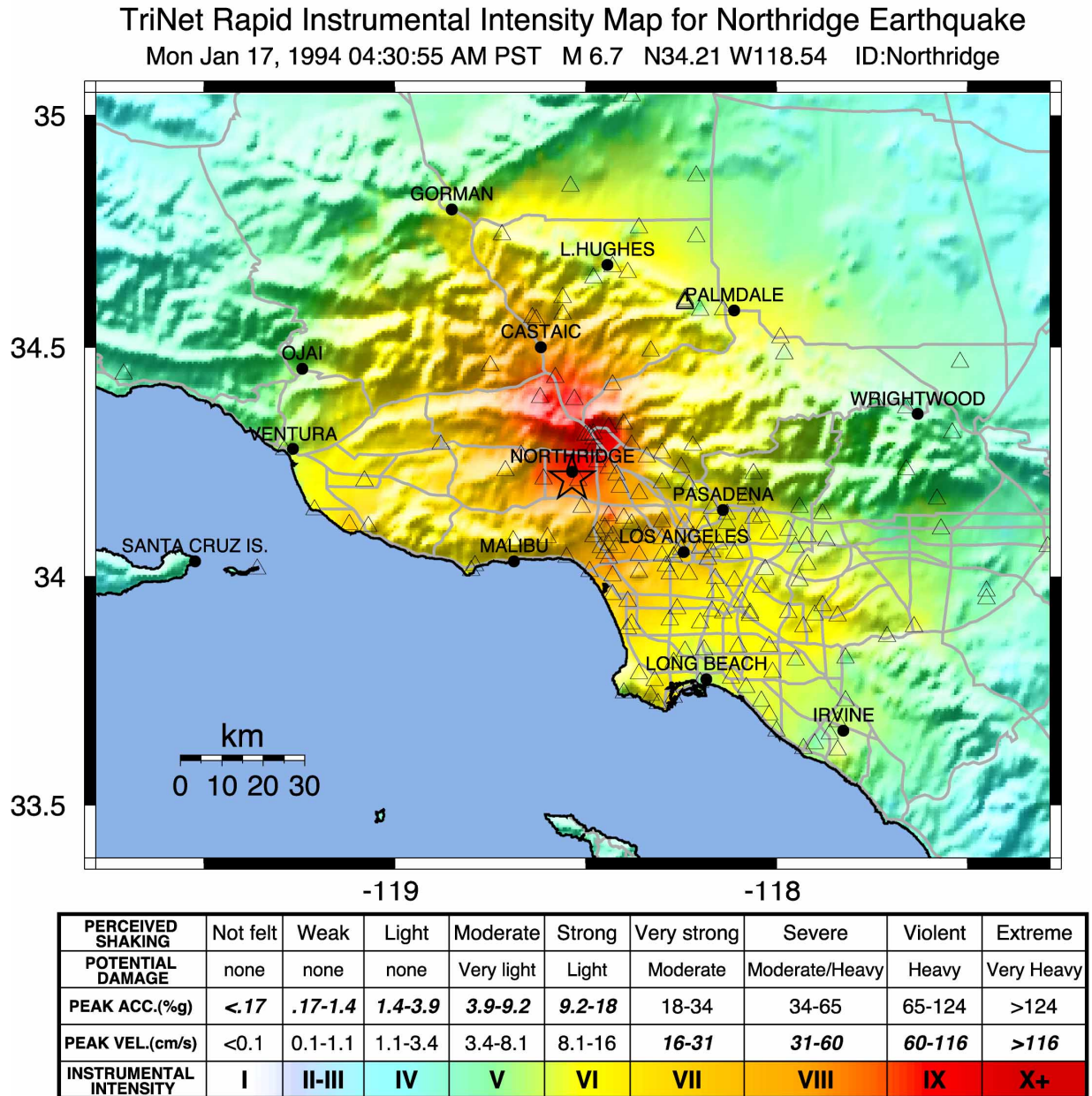


Figure 1. TriNet I_{mm} map for 1994 Northridge earthquake.

It should be noted that the TriNet ShakeMaps come with the important caveat that “[l]ocations within the same intensity area will not necessarily experience the same level of damage since damage depends heavily on the type of structure, the nature of the construction, and the details of the ground motion at that site.” [5]. This caveat, of course, naturally follows the historic development of Modified Mercalli

Intensity, that is, the rather ambiguous expressions of shaking experience by humans as well as characterizations of damage observed in various types of buildings and structural systems.

The authors studied the ambiguity implicit in the I_{mm} scale with regards to the performance of buildings using data from 1994 Northridge post-earthquake building inspections. Figure 2 shows the distribution of initial tagging type (green for “no damage”, yellow for “restricted entry”, and red for “unsafe”) for the buildings inspected in the greater Los Angeles area affected by the Northridge earthquake [6]. Out of these approximately 105,000 initial tags, the vast majority (95.2%) were green, 4.2% were yellow, and a mere 0.6% were red [7].

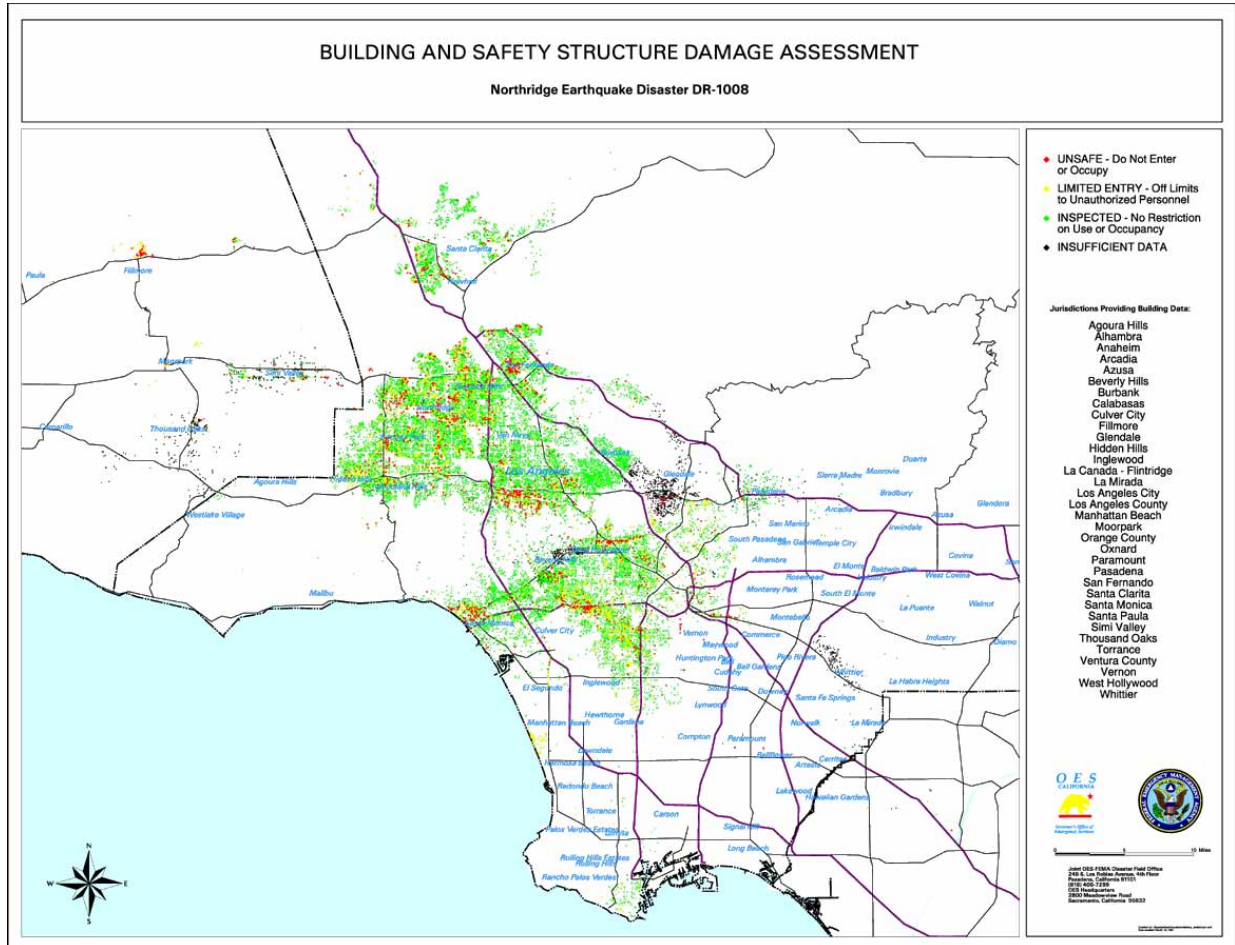
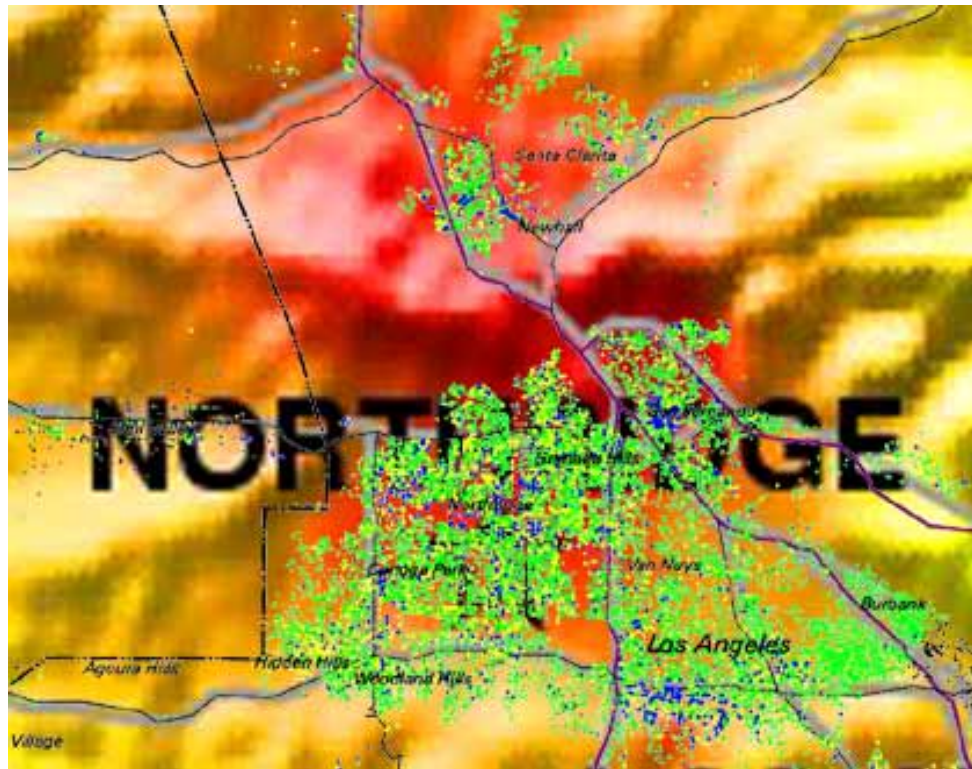


Figure 2. Initial building and safety structure damage assessment after 1994 Northridge earthquake: green = safe/undamaged, yellow=restricted entry, red=unsafe building [6].

When one compares Figures 1 and 2, it is seen that, expectedly, most of the red-tagged buildings were situated in areas that experienced higher intensity shaking. Rather more interestingly though, the overwhelming majority of the inspected buildings in these same high intensity shaking areas evidently sustained little or no structurally compromising damage and as such, were green-tagged. In other words, the overwhelming majority of the existing building inventory located in the most violently shaken portions of the region affected by the Northridge earthquake performed quite well. This fact can be clearly seen in Figure 3 which is an overlay of building tag-color data given in Figure 2 on the ShakeMap given in Figure 1. Note that in Figure 3, the red color for red-tag data points have been converted to blue to avoid blending in with the background intensity colors. The contrast between shaking intensity/projected damage

potential and actual building response as confirmed with field observations indicate rather obvious facts: 1) there is a need for a more refined shaking intensity measure that takes ground motion-building specific response interaction into account; 2) and, the apparent good performance of the existing non-conforming building stock brings into question the rationale of continually increasing code-based design spectra after every significant earthquake.



PERCEIVED SHAKING	Not felt	Weak	Light	Moderate	Strong	Very strong	Severe	Violent	Extreme
POTENTIAL DAMAGE	none	none	none	Very light	Light	Moderate	Moderate/Heavy	Heavy	Very Heavy
PEAK ACC.(%g)	<.17	.17-1.4	1.4-3.9	3.9-9.2	9.2-18	18-34	34-65	65-124	>124
PEAK VEL. (cm/s)	<0.1	0.1-1.1	1.1-3.4	3.4-8.1	8.1-16	16-31	31-60	60-116	>116
INSTRUMENTAL INTENSITY	I	II-III	IV	V	VI	VII	VIII	IX	X+

Figure 3. Building inspection/tag-color data (Figure 2 with “red”-tag changed to “blue”-tag to avoid blending in) overlain I_{mm} ShakeMap (Figure 1) for 1994 Northridge earthquake.

CONCEPT OF AN EARTHQUAKE ENGINEERING INTENSITY SCALE

Although peak ground motion parameters such as PGA and PGV as used in I_{mm} maps are useful yardsticks for measuring earthquake intensities, each earthquake has unique characteristics that greatly affect how particular structures respond to the ground motion. Illumination of the unique aspects of the interaction between shaking intensity and structures can be had by employing response spectra, thus providing the added dimension of period of vibration. To construct the link between peak response parameters and peak ground motion parameters, response spectra corresponding to I_{mm} scales can be approximated by applying dynamic amplification factors to the TriNet/ShakeMap regression PGA and PGV values given in the table

in Figure 1. Studies dating back from the 1970s to the present have provided recommendations for these amplification factors [8, 9, 10]. By multiplying the PGA values by the acceleration amplification factor for the short periods (i.e., constant acceleration range) and by multiplying the PGV values by the velocity amplification factor for the medium-to-long periods (i.e., constant velocity range), smooth response spectra for a chosen damping ratio can be formed to provide the basis for a structural response intensity scale, i.e., Earthquake Engineering Intensity Scale (EEIS) [11]. For this paper, since the relationships and examples used in this study are from California, the authors have selected amplification factors of 2.0 for the PGA and 1.7 for the PGV, which are similar to factors observed by Newmark and Hall [9] for the earthquakes in California and response spectra with 5% of critical damping ratio. Figures 4 and 5 illustrate the transformation of I_{mm} dividing intensity levels VIII and IX, and Figure 6 gives an EEIS template for the intensity range V to X. It should be noted that while the graph in Figure 4 is in the classical log-log tripartite format, i.e., in the form of pseudo relative response velocity (S_v) versus period (T), the graphs in Figures 5 and 6 are in the Acceleration-Displacement Response Spectra (ADRS) format [12], where spectral acceleration (S_a) and spectral displacement (S_d) form the orthogonal axes and radial lines represent periods (T). Note that the curved portions of the response spectra in ADRS format represent constant spectral velocities (S_v). It should be noted that the close correlation between shaking intensity and spectral velocities has been verified by Boatwright et al. [13] for the 1994 Northridge earthquake recordings and for period ranges not that different from those seen in figures in this paper.

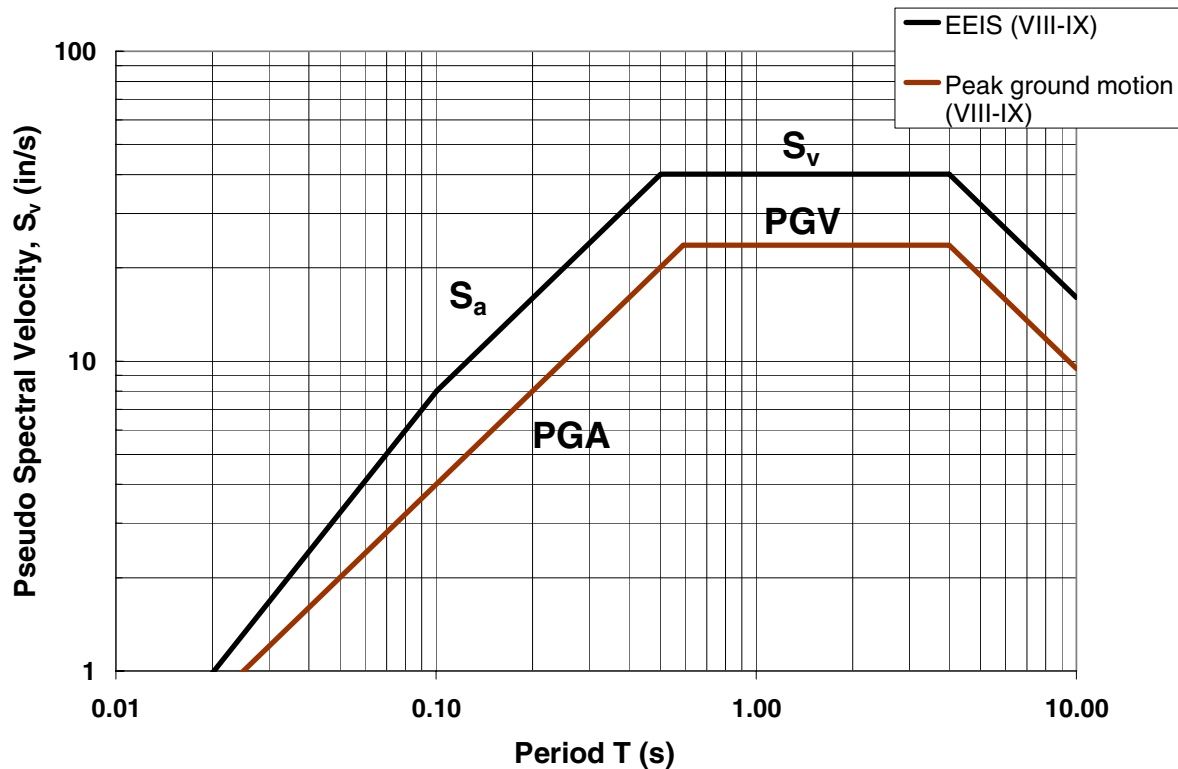


Figure 4. Example of transformation of PGA-PGV based Instrumental Intensity Scale (I_{mm}) to spectral response based Earthquake Engineering Intensity Scale (EEIS). Shown in log-log tripartite, i.e., pseudo relative response velocity (S_v) versus period (T), format.

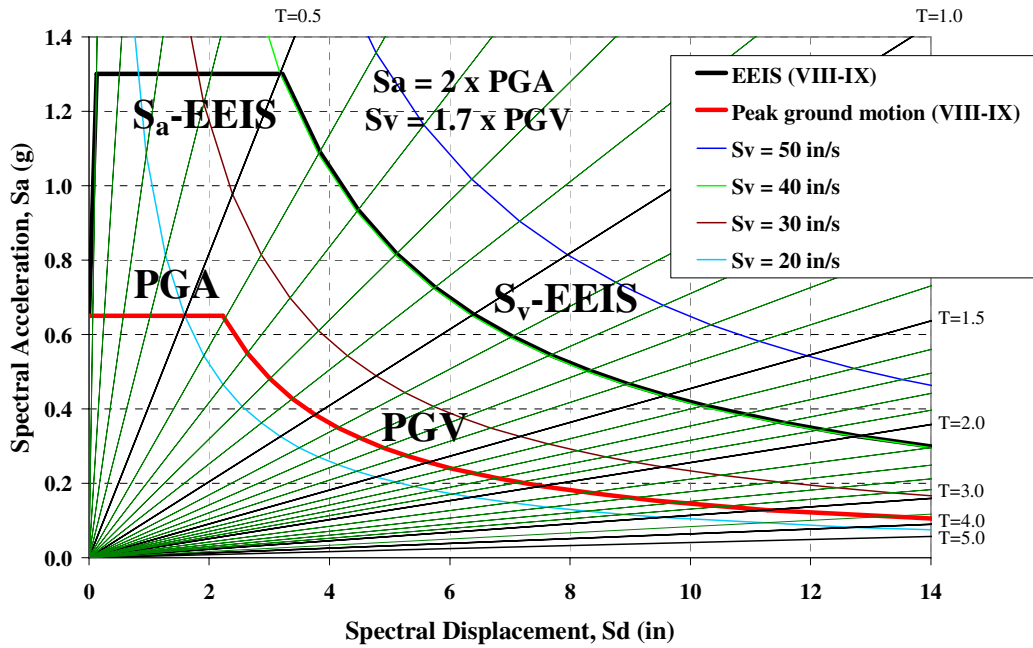


Figure 5. Graph in Figure 4 shown in Acceleration-Displacement Response Spectra (ADRS) format. Note that the radial lines emanating from origin of S_a and S_d indicate constant period axes, and that the curved lines indicate constant spectral velocities, S_v .

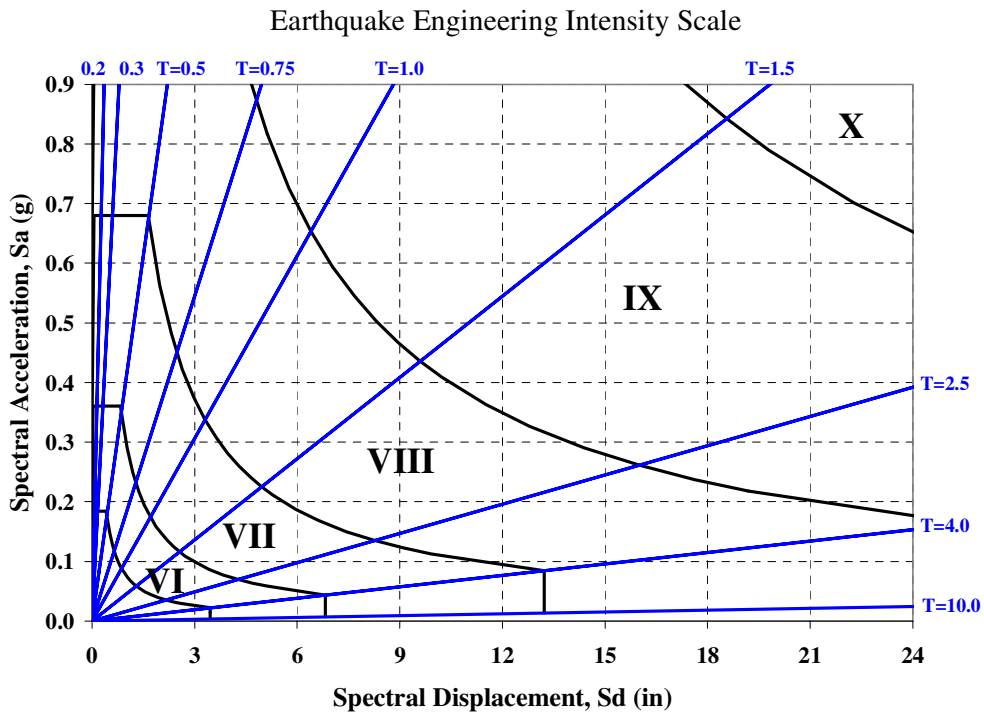


Figure 6. A template of Earthquake Engineering Intensity Scale (EEIS) based on Instrumental Intensity (I_{mm}) Scale used in TriNet (2.0 and 1.7 factors are used to obtain S_a and S_v from PGA and PGV, respectively.)

Illustrative Examples

Figures 7a-c illustrate the use of the template given in Figure 6 by superimposing on it the response spectra (5% damped) from three records obtained at instrumented sites during the 1994 Northridge earthquake in California. They represent the larger of two orthogonal horizontal ground motion recordings for Newhall, Sylmar, and Santa Monica sites [14]. Each of these recordings represents large PGAs, well over one-half gravity (g); but the shapes of the response spectra have markedly different characteristics. For example Newhall (Figure 7a) reaches into the intensity X around 0.7 sec and 1.2 sec periods, while Sylmar (Figure 7b) does so around 0.3 sec and 1.6 sec and Santa Monica (Figure 7c) does so around 0.2 sec. Newhall stays at the intensity IX up through a period of 2.5 sec, with a little dip to VIII at about 0.4 sec. Sylmar stays in intensity IX from 0.2 to 4 sec and Santa Monica drops below intensity IX at about 0.35 sec. It is also interesting to note the peak S_d values: Newhall at 24 inches at $T = 4$ sec, Sylmar at 30 inches at $T = 2.5$ sec, and Santa Monica at 14 inches at $T = 2.5$ sec. Figure 7d shows all three sites superimposed on one graph. The response spectra delineating between intensities IX and X tends to form an envelope covering all three sites.

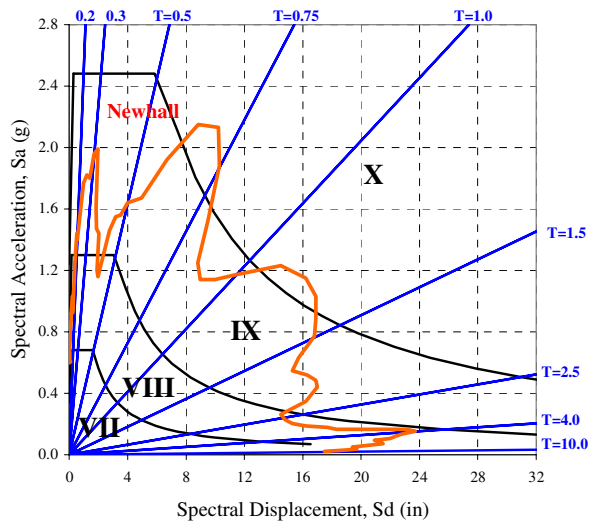


Figure 7a. Newhall, Northridge 1994.

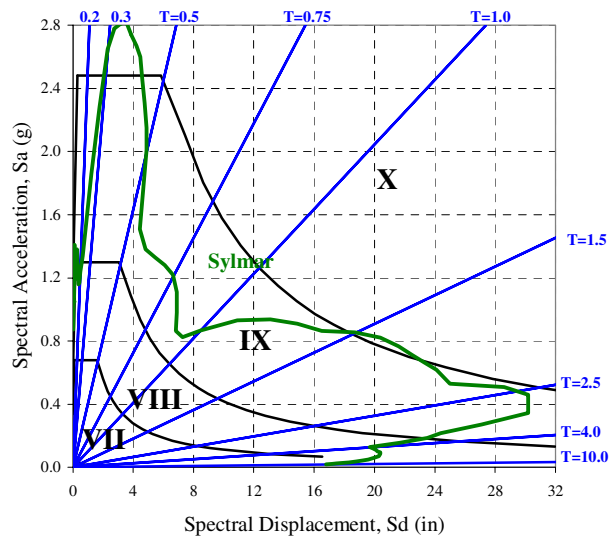


Figure 7b. Sylmar, Northridge 1994.

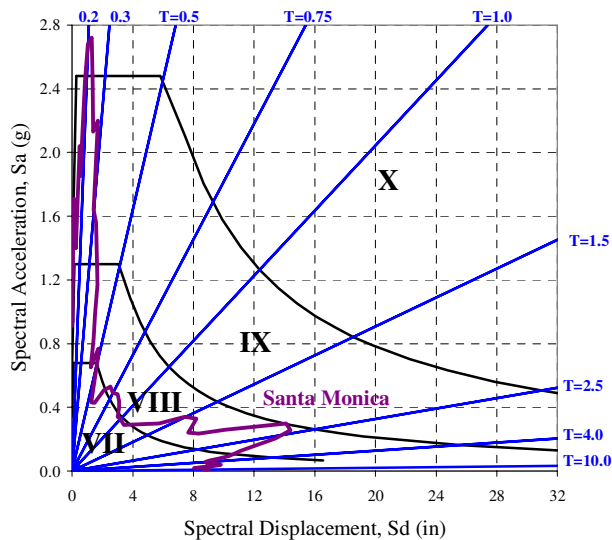


Figure 7c. Santa Monica, Northridge 1994.

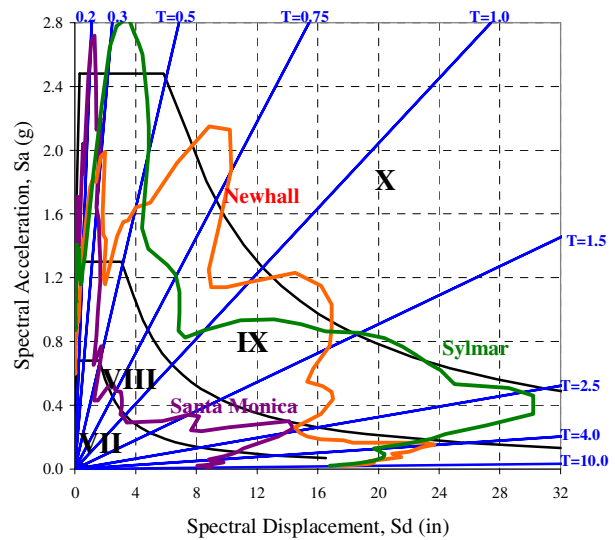


Figure 7d. Three Sites, Northridge 1994.

Incorporation of Capacity Spectrum Method into EEIS template

Capacity of building structures to resist earthquake ground motion can be illustrated by the use of so-called pushover curves that analytically track the horizontal force-displacement relationship of lateral force resisting systems that are pushed beyond their elastic limits. An example is given in Figure 8, where idealized pushover curves for five sample buildings designed to code in a study on code drift criteria [15] are superimposed on EEIS template. The curves represent a three-story steel braced frame building (short-period range), a three-story steel moment frame building and a 14-story concrete shear wall building (mid-period range), and a 15-story steel frame building and a 20-story reinforced concrete frame building (long-period range). Each curve is bilinear, where the mid-point represents the yield point and the end-point represents the nonlinear strength limit. It has been found that, for the code-designed short-period structure, yielding occurs at intensity VI while the strength limit is reached at intensity VII. For the mid-period and long-period structures, yielding occurs approximately at intensity VII while strength limit is reached at intensity VIII. It is worth contrasting this observation with the Northridge examples previously described, wherein it is clear that the overwhelming majority of structures that experienced shaking of intensity VIII, IX, and X survived with little enough structural damage to be re-entered and occupied. That analytical methods suggest collapse of large inventories of structures that survive nearly unscathed needs to be factored into future code development.

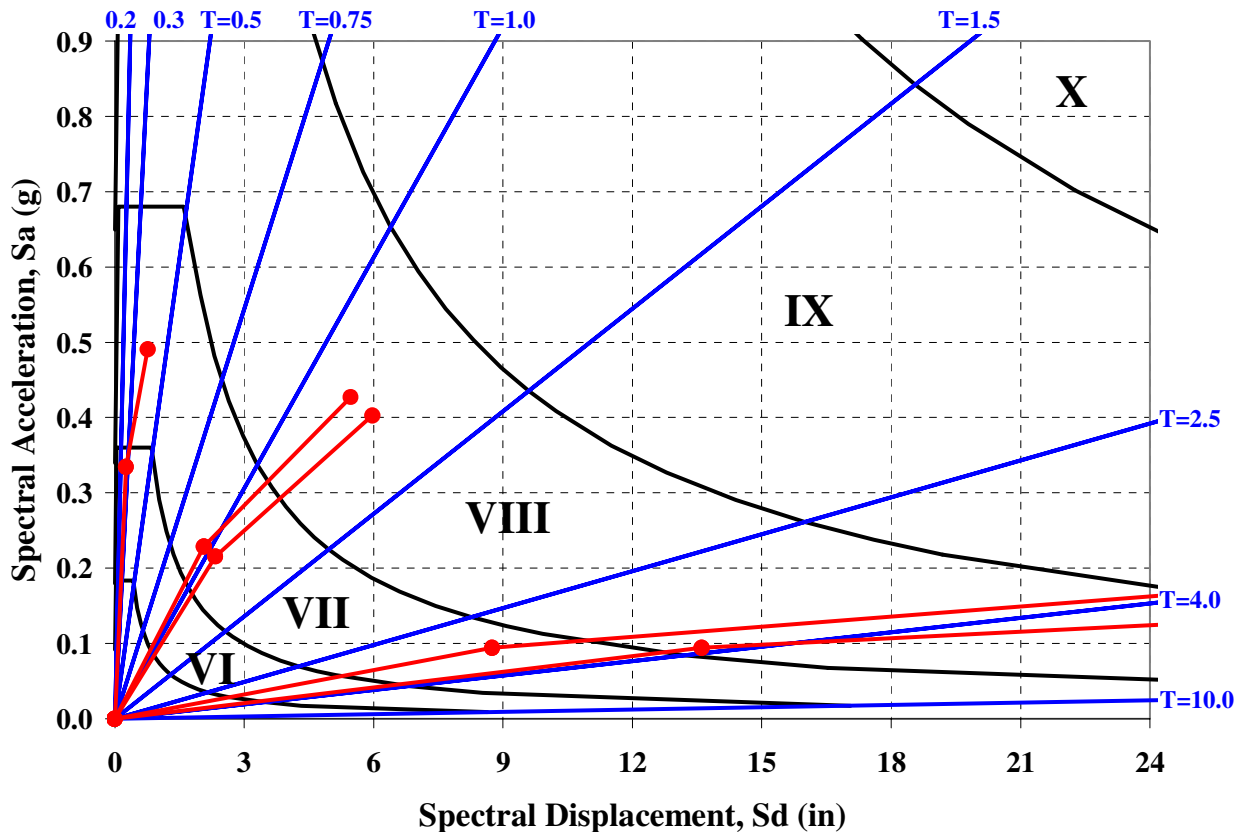


Figure 8. Sample 1997 UBC Zone 4 pushover capacities on EEIS template.

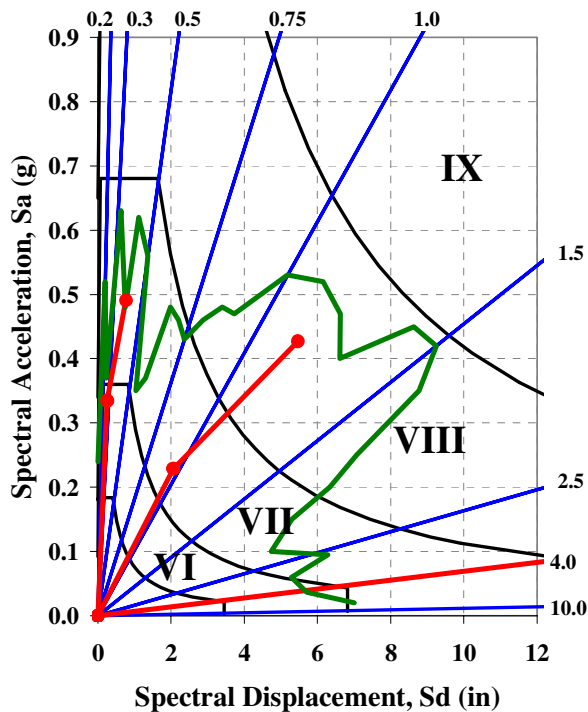


Figure 9a. Oakland, Loma Prieta 1989.

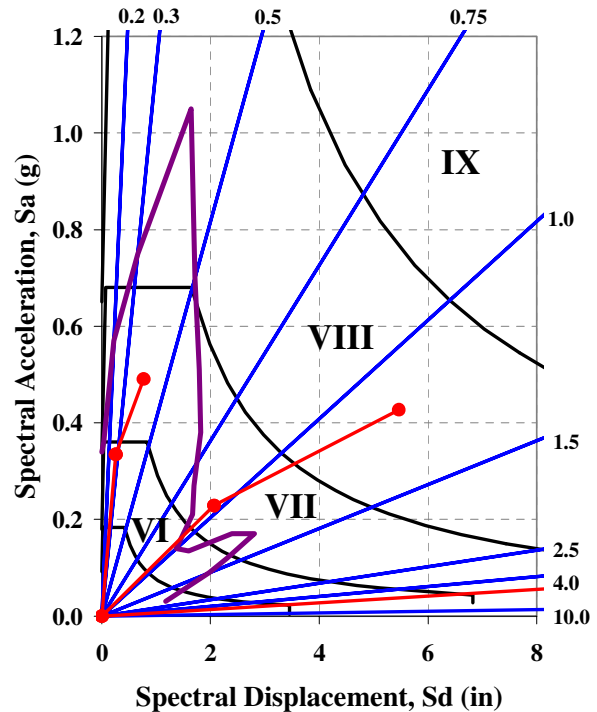


Figure 9b. Napa, Yountville 2000.

When the pushover curve of a structure is superimposed on response spectra, estimates can be made to evaluate performance by means of the capacity spectrum method (CSM) [16]. In Figures 9a and 9b, 5% damped response spectra from Oakland (Loma Prieta, 1989) [17] and Napa (Yountville, 2000) [18] sites are superimposed on the Figure 8 EEIS template with sample capacity curves. Note that Oakland had intensity VIII in the mid-period range and Napa had reached that intensity level in the short-period range. In other words, though it was moderately strong earthquake motion overall, Loma Prieta placed high demands on mid-rise buildings in Oakland. Yountville placed high demands on short buildings. Neither placed significant demands on high-rise buildings.

EEIS template to illustrate Design-Basis Earthquake

EEIS template can be utilized to study not only response spectra for actual ground motion records, but also proposed spectra such as those used in design codes. Figures 10 and 11 show 1997 UBC [19] design-basis earthquake spectra (DBE) superimposed on the EEIS template for soil classifications B and D, respectively. For soil class B, Zone 4 is in I_{mm} VIII, Zones 2b and 3 are in I_{mm} VII, and Zones 2a and 1 are in I_{mm} VI. At a softer soil class D site, the higher amplification of the ground motion places Zones 2b, 3, and 4 in I_{mm} VIII and Zones 2a and 1 in I_{mm} VII. This is consistent with the idea that ground motion will be more severe in soft soil sites.

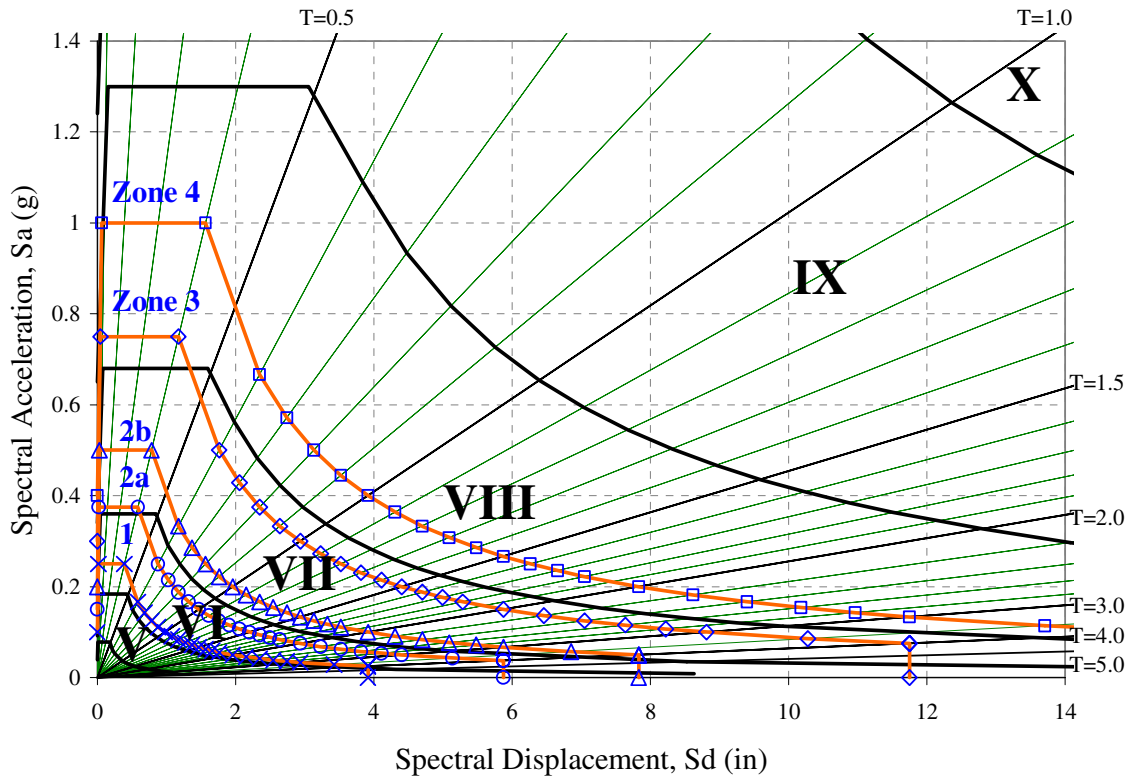


Figure 10. 1997 UBC soil class B (orange lines) on EEIS template.

For purposes of discussion, the Zone 4 DBE will be reviewed. If it is assumed that 1997 UBC code-compliant Zone 4 structures have yield thresholds at about 40% of the DBE (e.g., at the inverse of about $\frac{1}{2}$ the R-factor, where $R=5$), the building designed for soil class B may approach a yield limit at I_{mm} VI. The building designed for soil class D, which is designed for higher forces, may approach a yield limit at I_{mm} VII. However, most buildings were designed prior to the 1997 UBC where the soil amplification factors were less influential. As a rough approximation, I_{mm} VI and VII appear to be reasonably assumed initial damage thresholds, where well-designed buildings will experience limited or no damage and poorly designed can be expected to sustain damage. The authors note these are very rough estimates and that each intensity zone covers a high to low range ratio of a factor of 2. Furthermore, most buildings are generally more resilient than analyses suggest and often survive I_{mm} VIII with no observable damage [20]. For example, whereas the three Northridge sites shown in Figure 7d indicate earthquake response demands about equivalent to twice the UBC Zone 4, most buildings survived quite well and a great many were essentially undamaged. This can be explained in part by the fact that actual response spectra have irregular shapes with peaks and valleys while buildings are not perfectly linear-elastic and can suppress resonance effects by changing period and not absorbing energy.

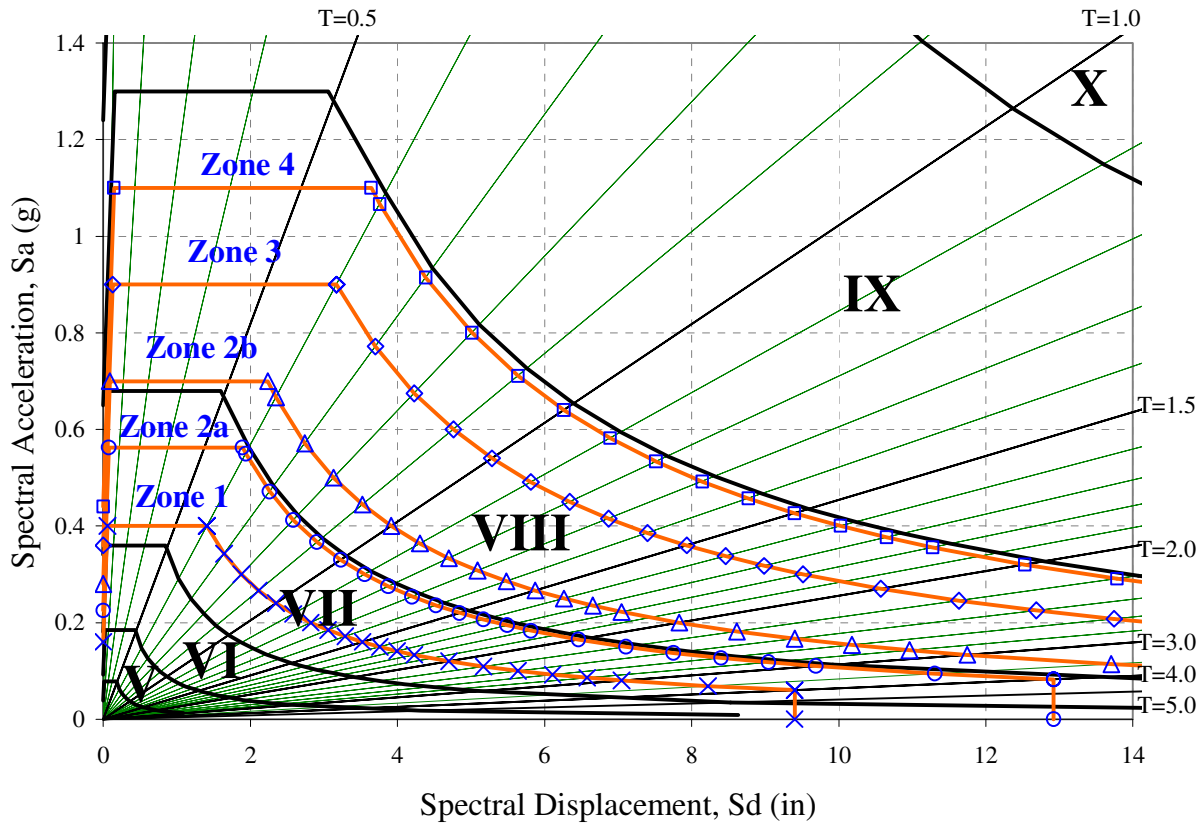


Figure 11. 1997 UBC soil class D (orange lines) on EEIS template.

Interpreting code design spectra

Using the approach explained in the previous section, design spectra from different codes could be projected on an EEIS template to facilitate comparison. Through Figures 12a and 12d, Uniform Building Code (UBC) pre-1976 through 1997 design spectra for Zone 4 at a site with soil class D are graphed to illustrate how the UBC design spectra evolved over the decades [19]. The response spectra, which correspond to the same structural system in the studied generations of UBC, are determined by adjusting the base shear coefficient V/W (ratio of base shear to weight of structure) to represent a spectral acceleration at the design strength level for a strength reduction factor equal to unity [20]. To give a sense of possible ultimate capacity ranges, curves that correspond to twice the code-demanded minimum design spectra are also drawn in Figures 12a through 12d. Use of EEIS template readily illustrates that, for example, there was a significant increase in code design spectra over the full period range in 1976. In 1988, however, the design spectra was modified in a such way that the constant acceleration range was extended resulting in a slight increase in design spectra for a narrow period range while mostly reducing the design spectra for long period range. In 1997, the constant acceleration range was once again extended. Furthermore, in 1997, the period-spectra relationship used in computing code design spectra has been modified to follow the well-known theoretical relationship, i.e., $S_a = S_v \cdot (2\pi/T) = S_d \cdot (2\pi/T)^2$ relationship. One sees this last modification in Figure 12d by observing the identical shapes of the constant pseudo-velocity spectra for the 1997 UBC and the constant pseudo-velocity intensity boundaries, which were obtained using the same well-known relationship between spectral quantities.

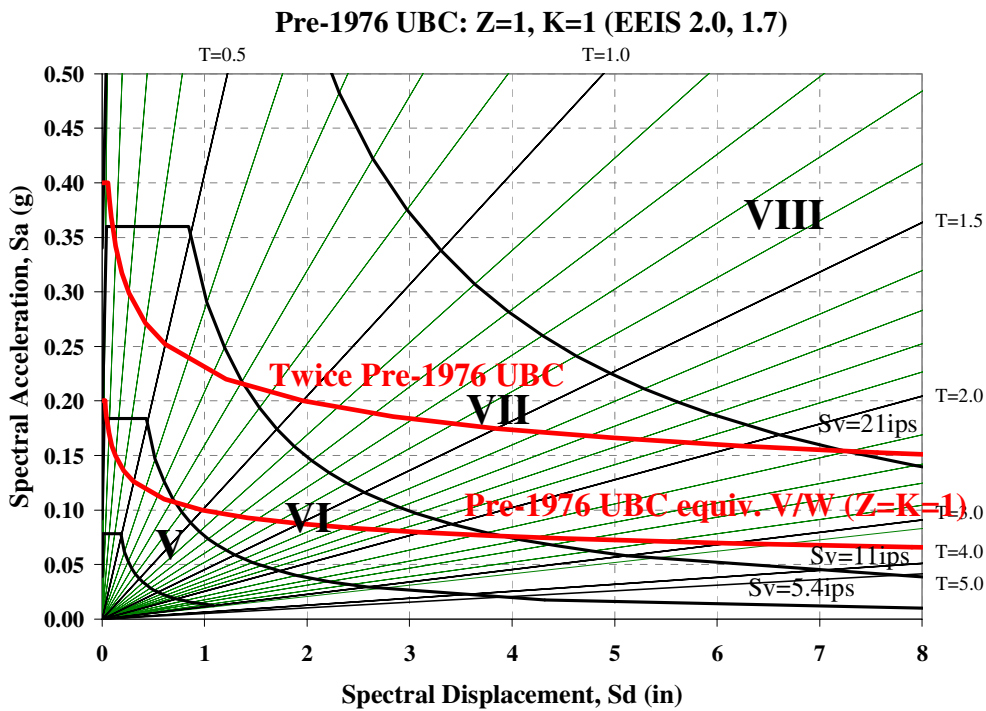


Figure 12a. Pre-1976 UBC Design base shear (red line) projected on EEIS template.

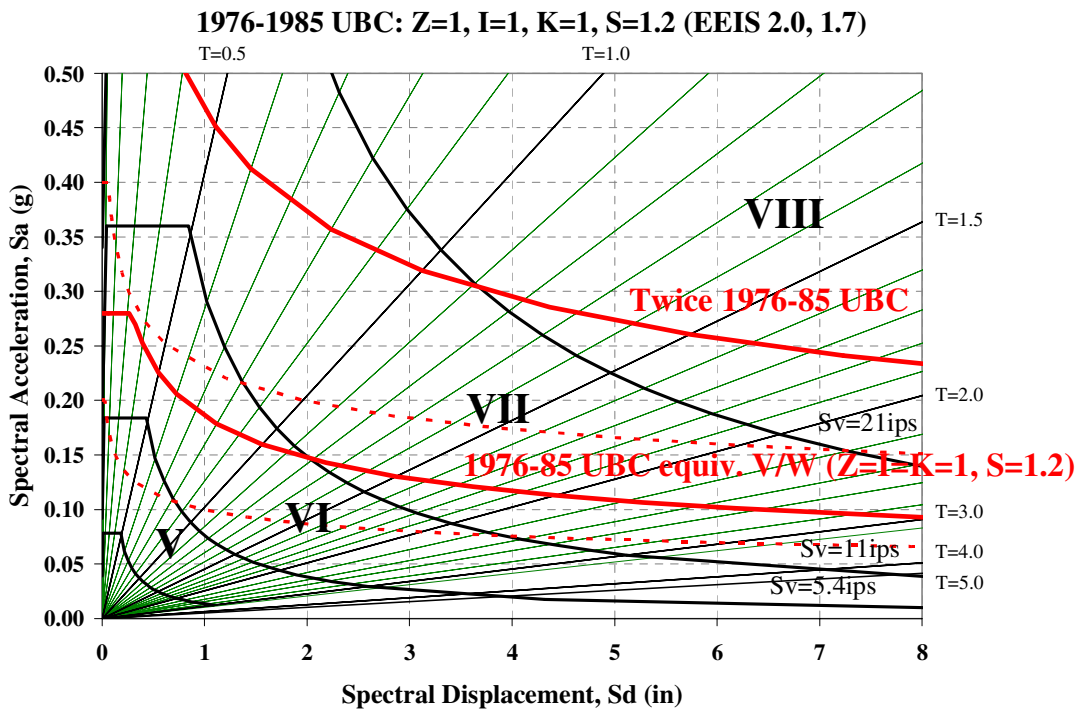


Figure 12b. 1976-1985 UBC base shear (solid red) projected on EEIS template. The dashed red lines show the previous generation, i.e., pre-1976, curves.

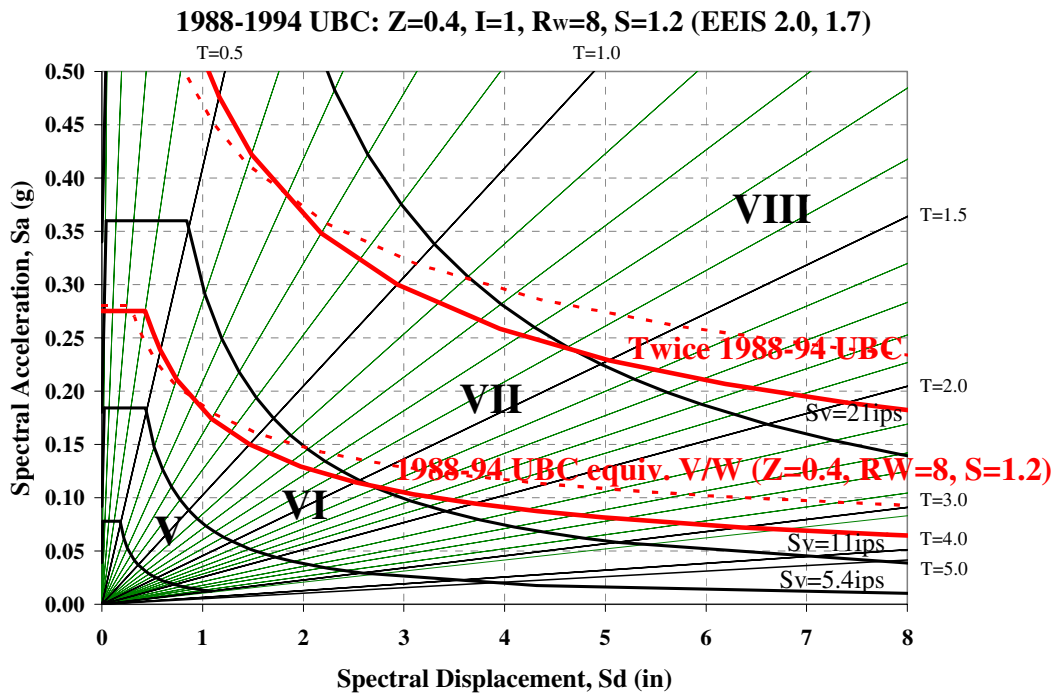


Figure 12c. 1988-1994 UBC base shear (solid red) projected on EEIS template. The dashed red lines show the previous generation, i.e., 1976-1985, curves.

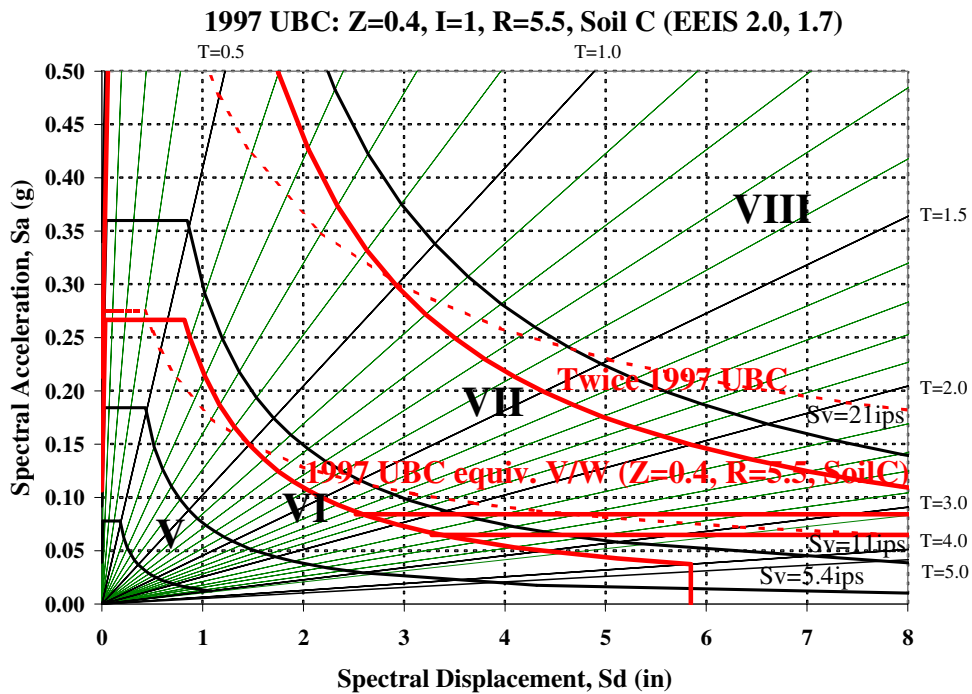


Figure 12d. 1997 UBC base shear (solid red) projected on EEIS template. Note that the horizontal red lines are code-specified minimum levels. The dashed red lines show the previous generation, i.e., 1988-1994, curves.

Further applications of the EEIS template

The authors believe that besides the uses illustrated above, the EEIS template could have other uses. For example, it could be assistance in improving the efficiency of rapid emergency response after an urban earthquake [21]. EEIS template provides a convenient medium include building response characteristics to estimate how particular building types are expected to respond to ground shaking and which ones are likely to be most susceptible in the affected areas. For example, the fact that high shaking intensities in short-period ranges affect one- or few-story buildings and high long-period intensities affect high-rise buildings could be incorporated into real-time ground shaking data evaluation for emergency response. Using a GIS database of the building stock in affected areas, an intensity distribution related to the built-environment could be obtained. Such intensity maps would increase the accuracy of real-time seismic risk/vulnerability assessments, and as such, increase the efficiency of post-event response. The same approach could be employed for scenario urban area earthquake simulations, too.

Since the EEIS template facilitates illustration of ground motion characteristics that relate to buildings, it readily allows incorporation of response information from instrumented buildings. Data from nearby instrumented buildings can be analyzed and integrated into response spectra predictions from free-field/ground motion recording stations. This integration will provide a reality-check on predictions of the shaking intensity and building responses.

CONCLUSIONS

The Earthquake Engineering Intensity Scale (EEIS) combines the concepts and information from Blume's Engineering Intensity Scale, TriNet/ShakeMap system, and the Capacity Spectrum Method. It provides a template that allows incorporation and illustration of various fundamental tools of earthquake engineering, such as, response spectra/demand spectra, building lateral capacity curves, and ground motion shaking intensity measures. The template facilitates visualization of response spectra showing characteristics of earthquake ground motion shaking and the potential damaging effects on various building classifications. The template can be used not only for rapid post-event building stock performance/vulnerability predictions, but also for scenario simulations. By allowing projection of a translated form of design spectra, instead of response spectra from earthquake ground motions, and by incorporating a building-specific estimated capacity curve, the EEIS template allows evaluation and prediction of the state of a building under code loads.

REFERENCES

1. Blume JA. "Engineering Intensity Scale for earthquakes and other ground motion." *Bulletin of the Seismological Society of America* 1970; 60(1): 217-229.
2. Richter CF. "Elementary Seismology." San Francisco: W.H. Freeman, 1958.
3. Wald DJ, Quitoriano V, Heaton TH, Kanamori H, Scrivner CW, Worden CB. "TriNet "ShakeMaps": rapid generation of peak ground motion and intensity maps for earthquakes in Southern California." *Earthquake Spectra* 1999; 15 (3): 537-555.
4. Wald DJ, Quitoriano V, Heaton TH, Kanamori H. "Relationships between peak ground acceleration, peak ground velocity, and Modified Mercalli Intensity in California." *Earthquake Spectra*, 1999; 15(3): 557-564.

5. TriNet. "ShakeMap disclaimers." <http://www.trinet.org/shake/disclaimer.htm>. Website accessed on March 2004.
6. Joint OES-FEMA Disaster Field Office, "Building and Safety Damage Assessment (Northridge Earthquake Disaster DR-1008) (Map)." Sacramento, CA: California Governor's Office of Emergency Services, 1994.
7. City of Los Angeles. "1994 Northridge earthquake (1994) data." Department of Building and Safety, City of Los Angeles, CA. 1994.
8. Newmark NM, Blume JA, Kapur K. "Seismic Design Spectra for Nuclear Power Plants." Journal of the Power Division 99 (PO2). ASCE, 1973.
9. Newmark NM, Hall WJ. "Earthquake spectra and design." Oakland, CA: Earthquake Engineering Research Institute, 1982.
10. Pujol S, Fierro EA, Freeman SA. "General characteristics of response spectra for records from South America." Proceedings of the 13th World Conference on Earthquake Engineering, Vancouver, Canada. Paper no. 1657. 2004.
11. Freeman SA, Paret TF, Irfanoglu A. "Structural implications of the TriNet Instrumental Intensity Scale." Proceedings of the 7th U.S. National Conference on Earthquake Engineering, Boston, Massachusetts. Oakland, CA: Earthquake Engineering Research Institute, 2002.
12. Mahaney JA, Paret TF, Kehoe BE, Freeman SA. "The Capacity Spectrum Method for evaluating structural response during the Loma Prieta earthquake." Proceedings of the 1993 National Earthquake Conference Earthquake Hazard Reduction in the Central and Eastern United States: A Time for Examination and Action. Oakland, CA: Earthquake Engineering Research Institute, 1993: 501-510.
13. Boatwright J, Thywissen K, Seekins LC. "Correlation of ground motion and intensity for the 17 January 1994 Northridge, California, earthquake." Bulletin of the Seismological Society of America, 2001; 91(4): 739-752.
14. Darragh, R, Cao T, Cramer C, Huang M, Shakal A. "Processed CSMIP strong-motion records from the Northridge, California earthquake of January 17 1994: Release No. 1." Report No. OSMS 94-06B. Sacramento, CA: CSMIP/CDMG, 1994.
15. Freeman SA, Searer GR. "Impact of the revised earthquake drift provisions on design and construction." Proceedings of the 69th Annual SEAOC Convention. Structural Engineers Association of California. 2000.
16. Freeman SA. "Development and use of Capacity Spectrum Method." Proceedings of the 6th U.S. National Conference on Earthquake Engineering, Seattle, Washington. Paper no. 269. Oakland, CA: Earthquake Engineering Research Institute, 1998.
17. Thiel CC, Jr. *Editor* "Competing against time. The Governor's Board of Inquiry on the 1989 Loma Prieta Earthquake." State of California, OPR, Sacramento, CA, 1990.
18. CDMG. Strong motion data center. <http://docinet3.consrv.ca.gov/csmip/>. Sacramento, CA: CSMIP/CDMG, 2000.
19. ICBO, "Uniform Building Code." International Conference of Building Officials. Whittier, California; 1973-1997.
20. Freeman SA. "Why properly code designed and constructed buildings have survived major earthquakes." Proceedings of the 13th World Conference on Earthquake Engineering, Vancouver, Canada. Paper no. 1689. 2004.
21. Freeman SA, Irfanoglu A, Paret TF. "Improving emergency response using building response data, ShakeMap data, and the Earthquake Engineering Intensity Scale." Proceedings of the 7th U.S./Japan Workshop on Urban Earthquake Hazard Reduction, Hawaii. Oakland, CA: Earthquake Engineering Research Institute and Institute of Social Safety Science (Japan), 2003.